

RESOLUTION IN ELECTRON MICROSCOPE AUTORADIOGRAPHY

IV. Application to Analysis of Autoradiographs

MIRIAM M. SALPETER, FRANCES A. McHENRY, and EDWIN E. SALPETER

From the Section of Neurobiology and Behavior, School of Applied and Engineering Physics, and the Department of Physics, Cornell University, Ithaca, New York 14853

ABSTRACT

The previous publications of this series described the expected grain distributions around model radioactive structures in EM autoradiographs as a function of the specimen resolution. This family of expected distributions was called the "universal curves". In the present study, experiments on ^{14}C -labeled specimens refine our information regarding the tails of the universal curves. When the expected grain distributions from ^{125}I -, ^3H -, and ^{14}C -sources were compared, significant differences were found depending on the energy of the isotope. These differences were primarily in the tails of the distributions, and are therefore important in correcting for cross-scatter when analyzing electron microscope autoradiographs.

Using the universal curves unique for ^{125}I , ^3H , and ^{14}C , we designed three sets of transparent overlays, or "masks", one set for each of these isotopes. The masks can be used by an investigator in a manner similar to that suggested by Blackett and Parry to generate grain distributions in autoradiographs on the basis of any desired hypothesis regarding the levels of radioactivity in different structures. A subsequent comparison between these generated distributions and those obtained from the observed grains in these autoradiographs leads to a determination of the most likely levels of radioactivity in the tissue. A computer (described in an Appendix by Land and Salpeter) can be used to find the "best fit" levels of radioactivity in complex cases. The accuracy of the masks was checked on generated line sources for each of the three isotopes.

KEY WORDS EM autoradiography · resolution · analysis of autoradiographs

Many studies have dealt with the problem of analyzing autoradiographs (1, 3, 10, 12, 14, 15, 17, 20, 23). Yet it remains one of the more troublesome aspects of EM autoradiography. The autoradiographic resolution is considerably poorer than the morphological resolution of the electron microscope, and thus a grain seen over a

specific organelle is not necessarily derived from a radioactive decay in that organelle. The task of analyzing EM autoradiographs is therefore to determine the most probable source for the developed grains. Although this cannot be done with any degree of certainty for a single grain, it can be done on a statistical basis for a population of grains accumulated from numerous autoradiographs. Once the source is identified, the amount of radioactivity can be assessed. At the root of

such an analysis has to be an understanding of the likely distribution of developed grains (radiation spread) around their parent radioactive sources. This information is contained in the resolution of the autoradiographic technique, which in turn depends on such parameters as the energy of the isotope, the specimen geometry, and the photographic process (1, 2, 6-9, 11, 13, 17-19, 21).

A decay from a radioactive source can produce a developed grain anywhere within a characteristic distance from the source. The resolution or the probability of finding a grain at different points within this distance can be expressed either in terms of a grain density distribution (grains/unit area, see Fig. 1) or in an integrated form (summed grains, see Fig. 2). The density distribution has frequently been used in defining EM autoradiographic resolution (6, 13). We have favored in our earlier papers a consideration also of the integrated form because it is easier to apply to analysis of autoradiographs. As with the density distribution, one can choose from the integrated distribution a single measure of resolution. We chose that distance from a radioactive source which defined an area with a 50% probability of containing a developed grain (or conversely, an area around a grain with a 50% probability of containing a source). This distance was called the half distance (HD) for a line source and half radius (HR) for a point source (17). (Values for HD are summarized in Table I.) Such 50% probability areas can be used to partially correct for radiation spread or cross-scatter in analyzing EM autoradiographs, for instance, in the probability circle methods (10, 15, 23).¹

Radiation spread can be accounted for more fully and accurately if one considers the full expected grain distribution around defined sources. The concept of the "universal curves" was introduced in the earlier papers of this series to facilitate this procedure. These curves were first based on the finding that, for a given source geometry and tritium labeling, the shape of the grain distribution was independent of the actual resolution or HD of the specimen. For instance, a 500-Å section coated with Kodak NTE emulsion has a

resolution (HD value) of 850 Å,² and a 1,000-Å section coated with Ilford L4 emulsion has an HD value of 1,500 Å (for other HD values, see Table I). Yet, although the width (or spread) of the grain distribution around a defined source depends on the HD, the shapes (and thus the mathematical descriptions) of the two grain distributions are the same. Therefore, when these grain distributions are normalized in distance units of their own HD, all the curves will coincide. These normalized distributions were then called the universal curves. The universal curves were first obtained for experimental line sources (17, 19, 21), as these were easiest to make experimentally. However, all extended sources, such as labeled cellular organelles, can be considered as collections of point sources randomly distributed over the entire area of that extended source. For each isotope, the universal curve for a point source was therefore derived mathematically and will henceforth be considered the primary universal curve. Such a curve can be used to generate the expected distributions for any extended radioactive structure by appropriate summation of the point source distributions, and becomes an obvious basis for autoradiographic analysis. This approach was used by Salpeter et al. (17) in the "grain density distribution" procedure, and by Blackett and Parry (3, 12) in the "hypothetical grain" procedure. Both procedures estimate the extent of radioactivity in a tissue by comparing the developed grain distributions observed in autoradiographs with the expected distributions generated from various assumed sources by the summation of point sources. We published a set of such expected distributions for regularly shaped structures and called these the families of universal curves (17). Blackett and Parry (3) provided a computer-generated list of random directions and distances derived from the point source universal curve, which can be used to generate the expected distributions directly on the autoradiographs. In the present study, we further extend this approach by designing transparent overlays (or masks) to facilitate generating expected grain distributions around assumed sources.³ In addition, we have

¹ Williams (23) has developed this "probability circle" procedure most elegantly. We feel that Nadler's application (10) is hampered by some incorrect concepts of resolution and a fallacy in the method for assigning shared grains.

² The Kodak NTE type emulsion is about to be released commercially in an improved form to be called either Kodak NTE2 or Kodak Type 129-01 (22).

³ After this paper was first submitted, but before it was resubmitted in revised form, a similar overlay procedure was published by Blackett and Parry (4). See Discussion.

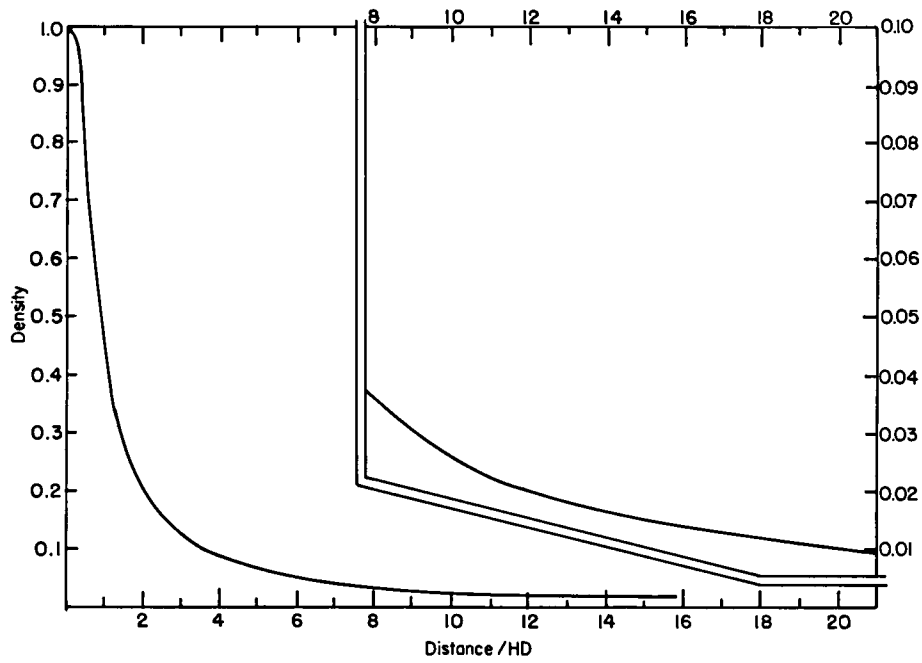


FIGURE 1 Full "universal" curve in units of HD for a ^{14}C -line source determined by combining the data from paper II of this series (21) and the new experimental data derived from the thick line source described here.

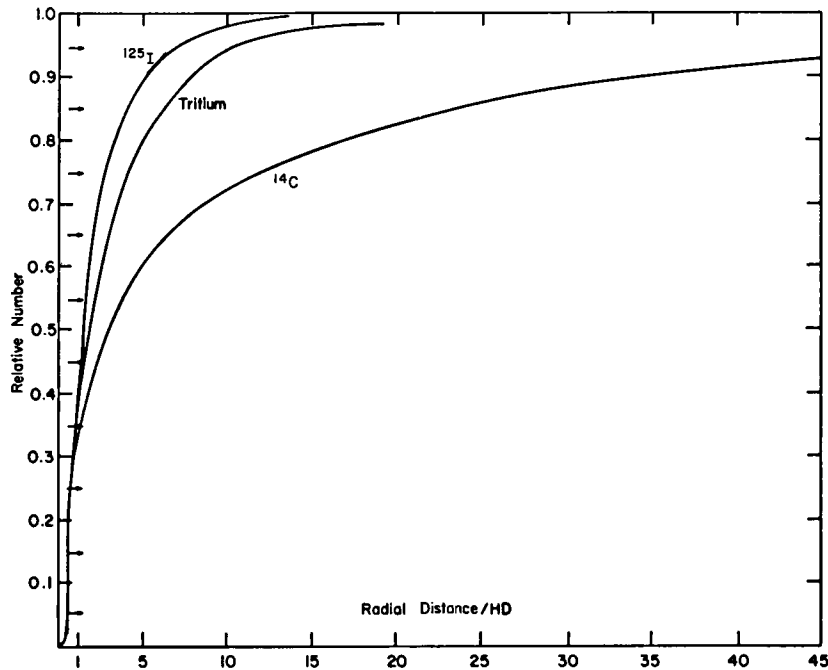


FIGURE 2 Integrated universal curves for point sources of ^{125}I , ^3H , and ^{14}C . The arrows on the Y-axis represent the midpoint of 10 consecutive bins containing an equal relative number of grains. The intersection of each arrow with the curves defines one of the 10 equal probability radial distances used in constructing the masks.

TABLE I
Selected Experimental Values for Half Distance
(HD)*

Emulsion	Section thickness λ	Isotope		
		^{125}I	^3H	^{14}C
Kodak NTE‡	500	500	800	—
mono-layer	1,000–1,200	500	1,000	2,000
Ilford L4	500	900§	1,300	—
mono-layer	1,000–1,200	900	1,500	2,300

* For greater detail, see References 17–19, 21.

‡ Applicable to Kodak NTE and NTE2 (see footnote 3).

§ Our ^{125}I HD is somewhat larger than that of Haworth and Chapman (9) but considerably smaller than that reported by Blackett and Parry (4).

|| A similar value was obtained for ^{55}Fe (11).

recently found that the shape of the universal curves depends on the energy of the isotope used (19). Thus, each isotope has a unique universal curve for a point source which differs particularly at the tails of the distributions. The higher the energy of radiation, the flatter and longer is the tail of the universal curve for the isotope. These differences are important if one wishes to make a full correction for radiation spread (or cross-scatter) among all the structures in an autoradiograph.

In this study, we therefore first determined experimentally the tail of the ^{14}C -universal curve which was previously not fully known. We then designed transparent overlays or masks for each isotope separately. These masks contain the information from the integrated curves in a form which lends itself to being transferred to EM autoradiographs for easy generation of expected grain distributions. The validity of these masks was tested by their ability to generate the known universal curves for each isotope. Some practical applications of these masks to the analysis of autoradiographs are discussed, and grain tabulations are proposed to maximize flexibility in hypothesis testing. Finally, a computer program for use in the most complex analyses is outlined in an Appendix (by Land and Salpeter).

MATERIALS AND METHODS

Experimental Determination of the Tail of the ^{14}C -Grain Distribution

The spread of radiation around a radioactive source

increases with the energy of the isotope. In respect to the three isotopes considered here, ^{125}I , ^3H , and ^{14}C , this spread is the largest for ^{14}C . (Data for ^{14}C are equally applicable to ^{35}S , as it has the same energy as ^{14}C .) In our earlier experimental resolution studies, grains were counted only to a "cut off" distance of 10 HD from the source for all isotopes. However, with ^{14}C , as with any isotope of energy higher than that of tritium, a full description of radiation spread should extend farther than 10 HD. In order to obtain enough grains for a statistically significant description of grain density beyond 10 HD, a thick line source was constructed in the manner previously used for the thin line source (21). The thick line source consisted of a 2,500- \AA layer of [^{14}C]polystyrene sandwiched between nonradioactive Epon and nonradioactive methacrylate, and then sectioned at right angles. EM autoradiographs of the line source were prepared by the "flat substrate" method of Salpeter and Bachmann (16), and the autoradiographs were exposed long enough to get significant grain counts up to 5 μm from the line. (The emulsion immediately above the line was thereby overexposed and could not be counted.) Grains were counted between 1 and 5 μm from the middle of this thick line source. Because in the earlier study on ^{14}C (21) the grains had been counted from the middle of the thin line up to a distance of 2 μm , we now had a 1- μm overlap between the thin and thick line tabulations. By combining the data from both studies, a full ^{14}C -grain distribution up to a 5 μm (or slightly >20 HD) cut-off distance was obtained. Fig. 1 gives the full ^{14}C -density distribution, plotted against distance from the line in units of HD. (HD for this specimen is $\sim 2,300$ \AA [Table I].)

Making of the Overlays or Masks

Mathematical formulae describing the density distributions for ^{125}I -, ^3H -, and ^{14}C -line sources have been refined and are given in paper III of this series (19). These lead uniquely to mathematical descriptions⁴ for the expected grain distributions around point sources. (The integrated curves are plotted in Fig. 2 in universal form, i.e., in units of HD.)

The purpose of the masks is to translate the information contained in the full integrated universal curve to the situation existing in autoradiography. Essentially, in an EM autoradiograph there are many point sources each on the average giving rise to, at most, one developed grain. Therefore, in the masks we made a set of point sources and to each we assigned a single grain whose distance from the source was chosen randomly from 10 equally probable distances on the integrated distribution. Thus each "source-to-grain" pair had an equal probability of occurrence. How this was done can be seen in Fig. 2.

⁴ These mathematical descriptions (in Appendix C of reference 19) have a misprint in Eqs. 6–9. The quantity denoted as "a" should be parameter "C" (numerical values are given in Table A of reference 19).

For example, 10% of the grains from a ^{14}C -point source (e.g. 0–0.1 relative number) fall between 0 and 0.5 HD from that source, and another 10% (e.g. 0.5–0.6 relative number) fall between 2.5 and 5 HD from that source. Thus, a grain has an equal probability (10%) of being between 0 and 0.5 HD or between 2.5 and 5 HD from a ^{14}C -radioactive decay. We can thus think of a point source as having a series of concentric annuli around it, each of different width but each containing 10% of total grains. The 10 arrows on the Y-axis of Fig. 2 define the midline of such annuli. Because the direction taken by the emitted particle is random, the grain can be anywhere in the defined annulus. Thus, in constructing the six masks for a given isotope, the direction and distance of each grain from its source were determined by a random choice from among 160 equally probable grain positions. Each involved a random choice of one of 16 possible different directions, and one of the 10 equally likely radial distances marked by the arrows in Fig. 2. Figs. 3–5 show these overlays in reduced size.

For any desired magnification of the autoradiographs to be analyzed, investigators can make their own overlays by photographing Figs. 3–5. The set for the specific isotope can then be magnified photographically so that the 10 HD bar matches what 10 HD would be for their autoradiographic specimen at whatever final magnification they prefer. (See Table I for sample HD values.) Vu-foil transparencies can then be made from the photographed masters. It is of course easiest to decide on one or two useful magnifications, make the masks, and then print all autoradiographs at those magnifications. In Figs. 3–5, we indicate for each isotope one useful magnification for a set of 8×12 -inch masks as well as the HD values applicable for 1,000-Å sections and monolayers of either Ilford L4 or Kodak NTE emulsion.²

Validations of Masks

To determine that no errors were committed in constructing the masks, we tested to see whether with their use we could generate the expected grain distribution from an assumed source. We chose a line source because in our earlier studies on resolution real experimental grains were obtained for such a source and accurate universal curves derived from it. The expected grain distributions were generated as follows. For each isotope, four straight lines at varying angles to the horizontal plane were drawn on a page. 144 equally spaced hypothetical point sources (to be called generated sources) were punched along each line with a needle. All six “masks” per isotope were then used to generate grains from these linear sources. The edges of each mask were always kept parallel to the edges of the page, but the mask was moved so that a different mask source was laid, in consecutive order, over each generated source along the line. A hole was then punched into the page through the center of the X marking the generated grain paired to that particular source. The nearest distance from each generated grain to the line was recorded. The data were tabulated in histogram

form to provide generated grain density distributions with distance from the line, as was done for the developed grains in the initial resolution studies (papers I to III) of this series (17, 19, 21). If the masks are valid, the histograms of generated grains should match those of the experimental grains, and thus should reproduce the universal curve for a line source. Fig. 6 shows that for each isotope there is a good match between the generated grain histograms and the universal curves for a line source. We should note that the mathematically derived universal curve is more accurate than the mask generated histogram.

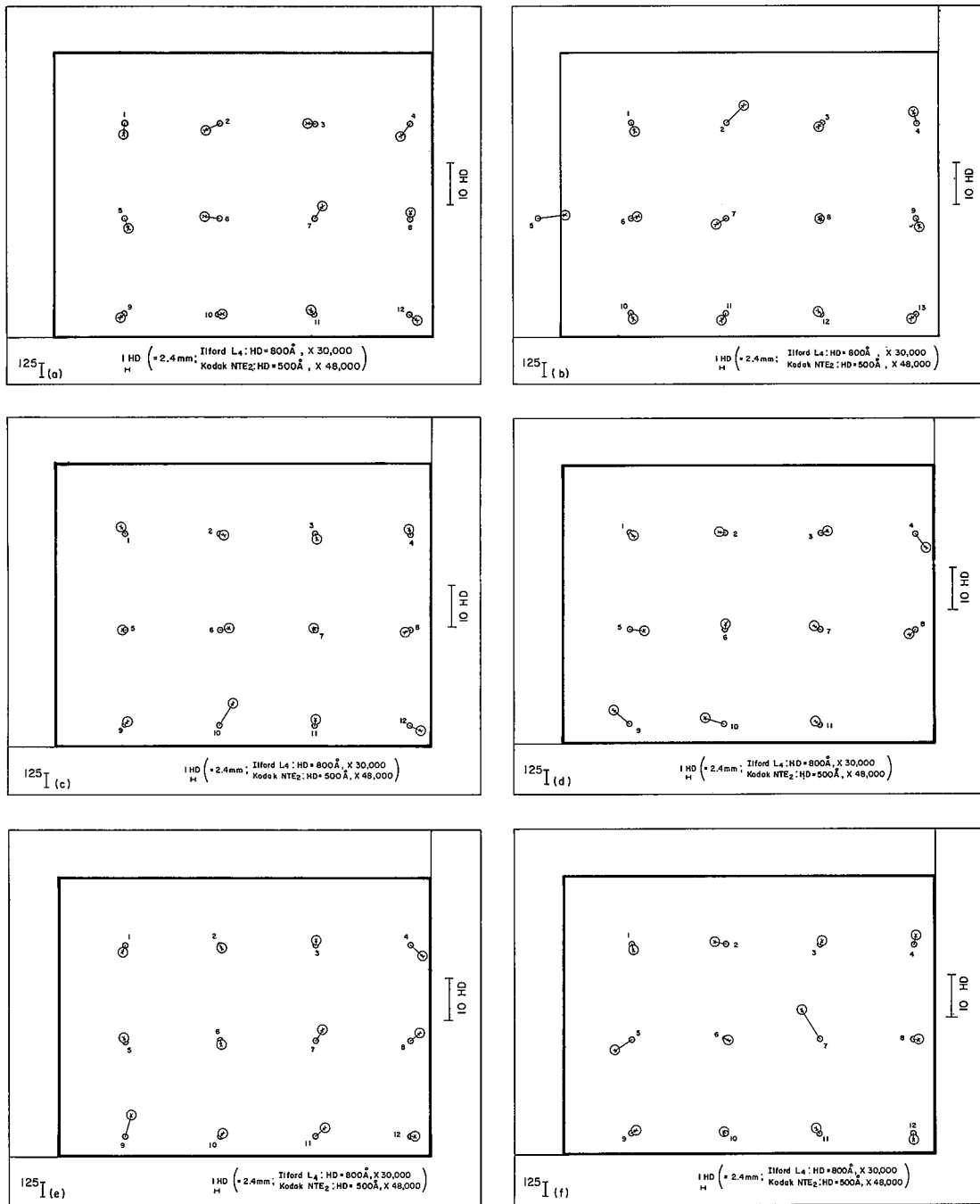
RESULTS

Use of the Masks

The masks can be used in any of four orientations. As shown in Figs. 3–5, the source points are not symmetrically arranged within the center rectangle, and the source-to-grain pairs fall on different parts of a print depending on whether the top left corner of the mask is lined up with the top left or with the bottom right corners of the print, and whether the mask is turned over (i.e., the numbers mirror imaged). For each isotope, the six masks thus give 288 different source-to-grain pairs.

Before proceeding with a detailed description of EM autoradiographic analysis by means of the masks, we should explain some terms to be used in this study. The term “observed grains” refers to the real developed silver grains in the autoradiograph. The mask tabulation provides a set of “generated” source-to-grain pairs. The generated grains then serve as a basis for subsequent computations based on various hypotheses which result in a set of “computed” optimized sources and “computed” expected grains.

The term “source compartment” defines the location of generated or computed sources, and the term “grain compartment” defines the locations of observed, generated, or computed grains. Before beginning a tabulation, the investigator must decide on an initial set of source and grain compartments. These may subsequently be altered if the initial results so indicate. By definition, a single source compartment will always be considered as a uniformly labeled structure, i.e., one consisting of randomly distributed point sources as some overall level of radioactivity. A source compartment can be coincident with a cellular organelle such as the mitochondrion, etc. but it need not be. It could be, for instance, a 1- μm band inside the plasma membrane of a cell. Such a source compartment, if it exists, is not easy to



FIGURES 3-5 Masks (overlays) for three isotopes: ^{125}I , (Fig. 3), ^3H (Fig. 4), and ^{14}C (Fig. 5). In its final form, each of the six masks contains, on the average, 12 source-to-grain pairs numbered consecutively, arranged in a two-dimensional pattern. Each source-to-grain pair consists of a source (center of small circle) connected by a line to a grain (x) generated from it. (A circle of 1-HD radius was drawn around each grain as an aid in tabulation.) For each isotope, the HD value for a 1,000- \AA section and Ilford L4 or Kodak NTE emulsions is indicated. The magnification for a 8×10 print is also indicated. The inner frame was constructed to allow for radiation-spread correction between the printed autoradiograph and areas outside it. In the analysis, one should count only those observed real grains that are found in the autoradiograph within the small rectangle of the mask.

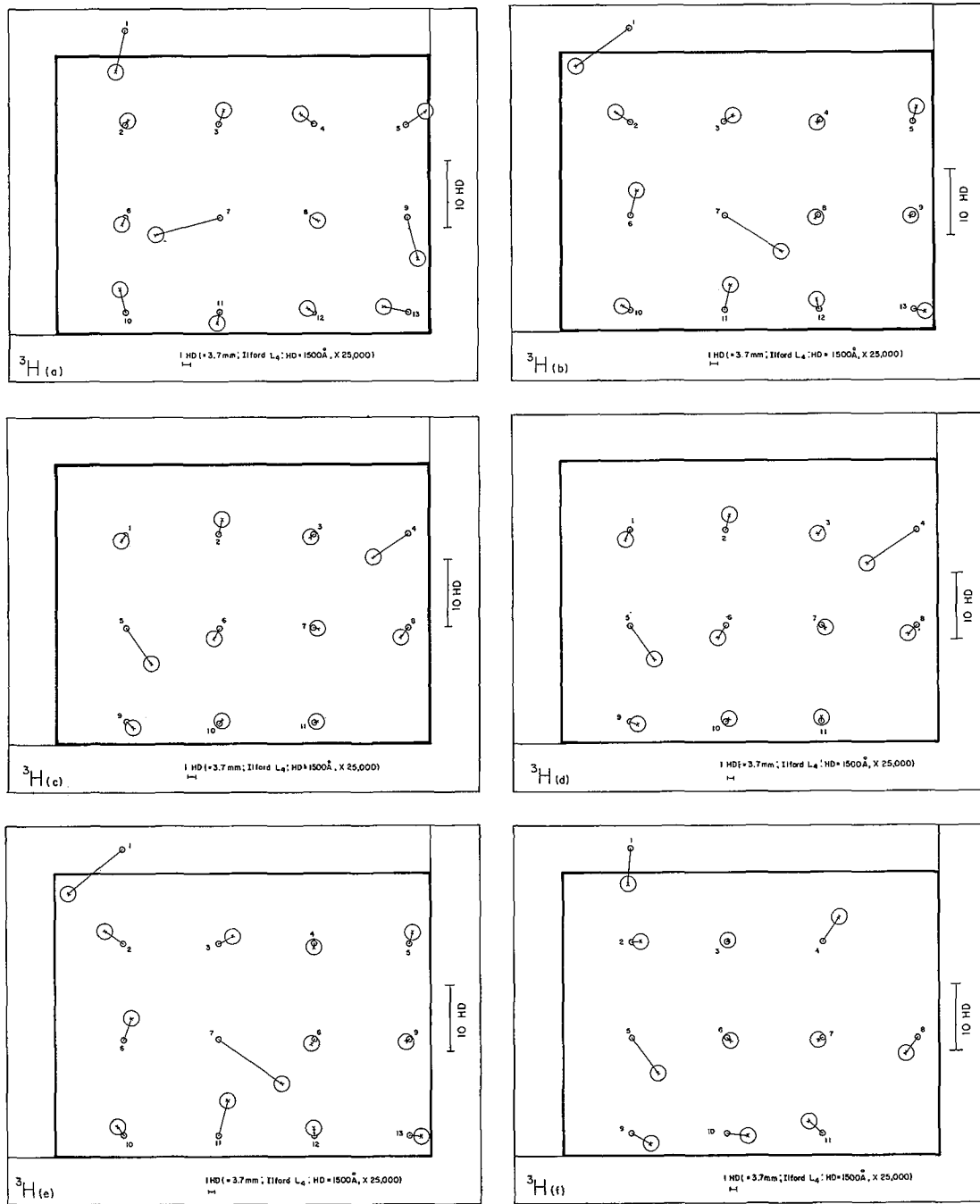


FIGURE 4

choose initially without some prior knowledge or preset hypothesis, but may emerge with iteration during the analysis.

The chosen grain compartments should be geometrically related to the source compartments. The grain compartment for any given grain can

be identified in a variety of ways, and depends to some extent on the mode of grain tabulation used. However, it must be remembered that the same grain compartments and mode of tabulation must be used for the observed as for the generated grains. In some modes the center of the grain is

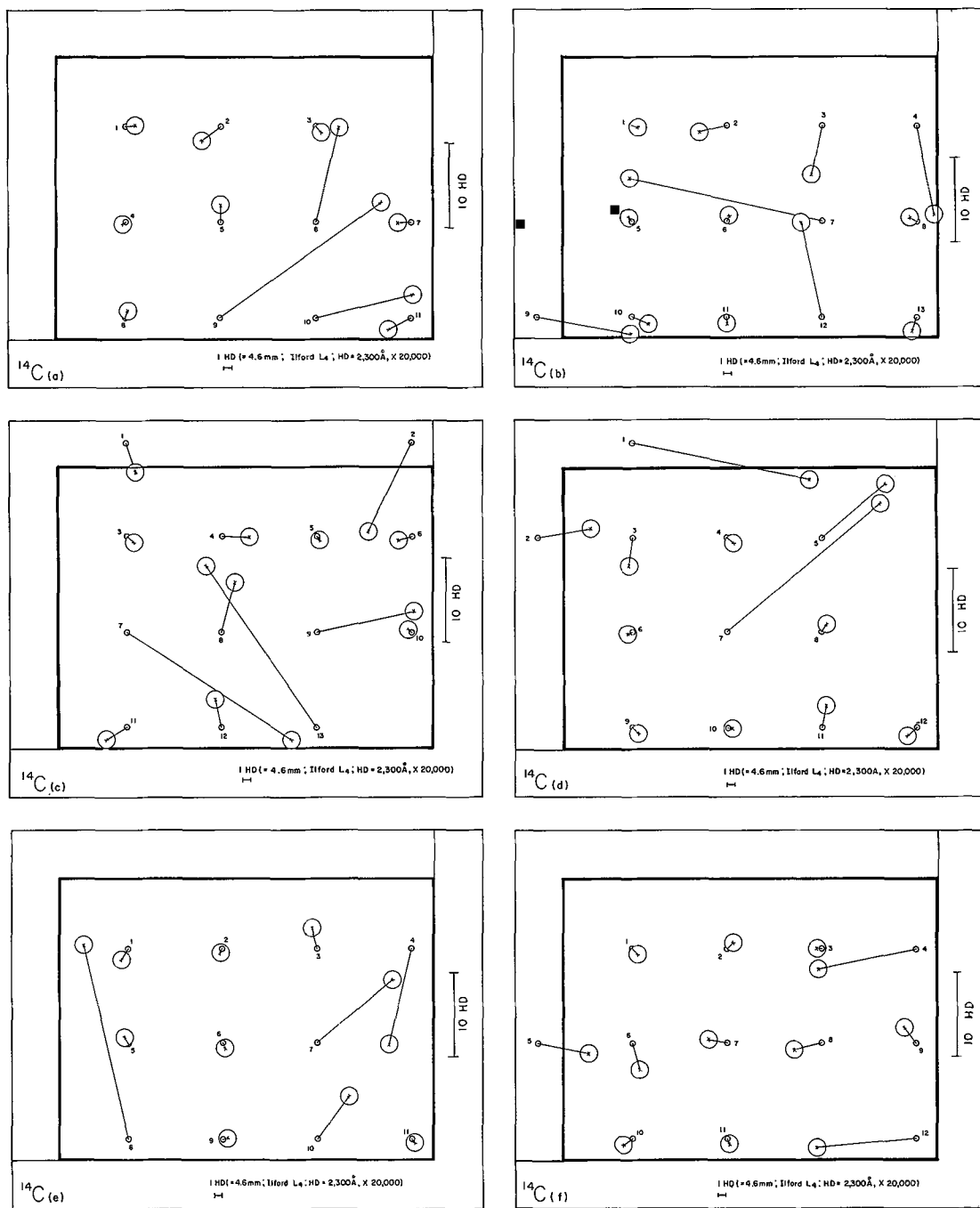


FIGURE 5

first marked, and the grain is considered to be in that grain compartment over which this center lies. Alternately, the distance from the grain center to a defined structure (usually some source

compartment) is tabulated in histogram form, and each histogram column then is a separate grain compartment. In another mode of grain tabulation, a circle of defined size is drawn around the

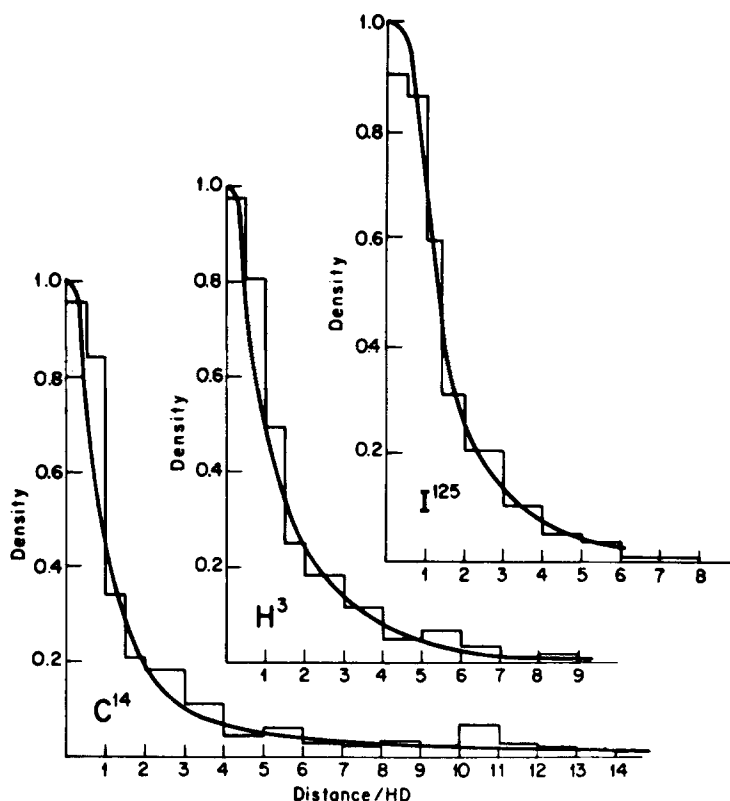


FIGURE 6 Histograms, plotted in units of HD, give grain distributions generated by use of the masks from assumed line sources labeled with ^{125}I , ^3H , and ^{14}C . The smooth curves represent the universal curves for a line source labeled with these isotopes. The good fit provides a validation of the masks.

grain and the grain is located according to what structures fall within that circle. The circles provide an easy mechanism for identifying a grain compartment outside a defined structure such as a rim whose width is equal to the radius of the circle. This circle mode of grain tabulation is used in the probability circle analysis, and has been adopted in the hypothetical grain analysis of Blackett and Parry (3, 12). We prefer to use all three modes of grain tabulation singly or in combination in the mask analysis to increase the flexibility in subsequent hypothesis testing. Locating grains by their centers is simplest, and recommended when the chosen grain compartments are large structures or are histogram columns. Histogram grain compartments are optimum when the related source compartments are small (e.g. a line), or potentially highly radioactive. The use of circles around grains is preferred if small structures are under consideration and histograms are not used. As will be justified, it is generally

more reliable to have a larger number of different grain compartments than of source compartments.

Once the source and grain compartments are chosen, the observed grains are tabulated in relation to the grain compartments, and the mask generated source-to-grain pairs in relation to both the source and the grain compartments as follows: numerous EM autoradiographs representing a random or systematic sampling of the tissue of interest are analyzed. The masks are laid over the autoradiographic prints in one of the several orientations as previously indicated (see Fig. 7). For each source-to-grain pair, one then records the source compartment containing the source and the grain compartment containing the grain.

Because the mask sources are sparsely spaced to avoid clutter (in an 8×10 mask we have one source per 4 square inches), the probability may be low that a mask source will fall on small or rare compartments. To improve the statistical

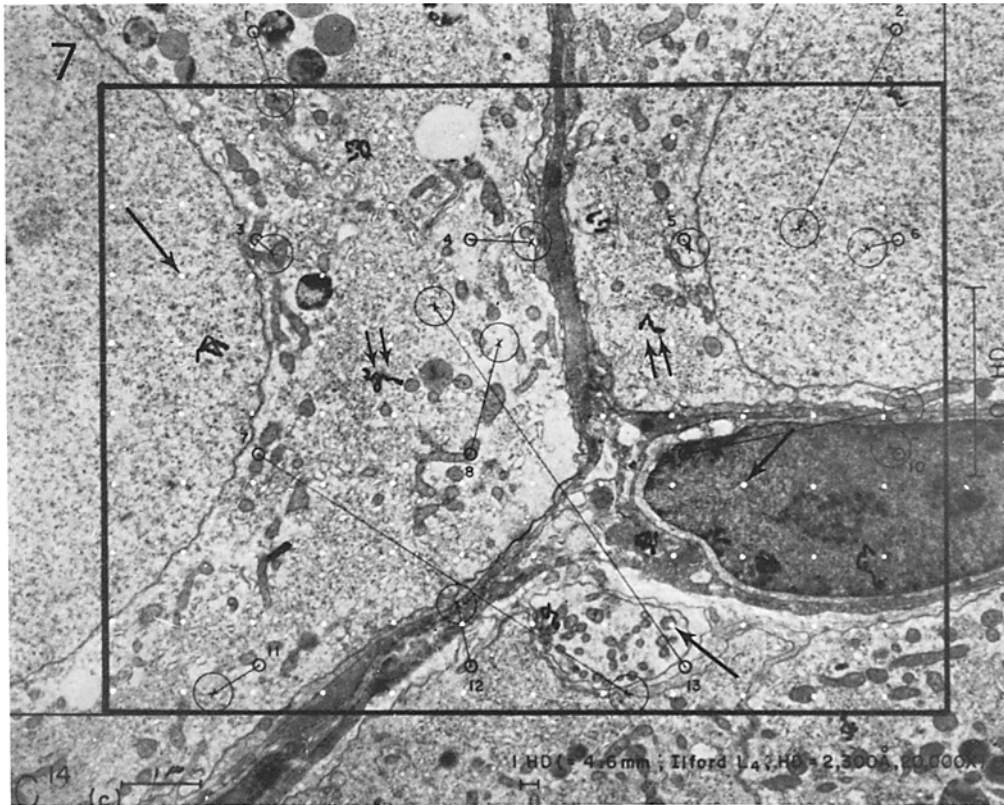


FIGURE 7 Sample autoradiograph with a superimposed ^{14}C -mask. Double arrows point to real observed developed grains. The generated source-to-grain matrix derived from many such autoradiographs is given in Table II *a*. The single arrows point to holes punched into the autoradiographs for tabulating small and rare source compartments which otherwise would not have enough generated sources to fulfill the required ratio of generated grains to observed grains. In the example illustrated here, only the axon source compartment was tabulated using the generated sources from the punch hole spacing, as well as from the regular mask source spacing. Note that in Table II *a*, all grains generated from the axon source compartment (row 5) have been divided by 10, as the punch hole density was nine times higher than the mask source density and both were used once on this print.

sampling of such small structures, we have devised a grid consisting of closely spaced nails held in square array in a rigid sheet of plastic. When this grid is used, the nails are pressed through an autoradiographic print (see legend to Fig. 7). Only those punch holes that are seen over the small structure of interest are used. All other punch holes can be ignored. A mask is moved so that one of its sources is placed over each nail hole (a different source per hole), as was done for the holes punched along the lines used in validating the masks. Each punch hole thus serves as the location of a source from which a grain is generated. Each source-to-grain pair is then tabulated in a source and grain compartment as previ-

ously outlined. By adding the punch holes to the mask sources for small structures only, the statistical sampling of the small compartment is enhanced without needing excessive sampling on the large structures. To maintain the same unit of source density for all compartments, the grains derived from source compartments for which both punch and regular mask sources were used must be divided by the overall increased source density (e.g., see legend to Fig. 7).

To sample a linear source, hypothetical sources can be placed along the linear structure which are then used in conjunction with the mask to generate random grains. These grains would then be tabulated in the same way as those generated

from other sources. However, the final units of source density must be expressed per length of line rather than per area of compartment.

In doing the mask tabulation, all six masks should be used in each of the four orientations before starting the sequence again so that the full universal curve is reproduced most accurately. All grains and sources must be accounted for in some compartment. Finally, before any division for the purpose of equalizing generated source density, at least three to five times as many generated grains as observed grains should be obtained in the total analysis, and at least two to three times as many generated grains as observed grains should be obtained for every compartment tabulated. This insures that the observed grain sampling and not the generated grain sampling is the limiting factor determining the statistical accuracy of the results. The mask generated source-to-grain pairs are then tabulated in matrix form as illustrated in Table II *a*. (Having more grain compartments than source compartments, i.e. as in Table II *a*, gives a nonsquare matrix, whereas having an equal number of grain compartments and source compartments gives a square matrix.) In Table II *a*, we also see the number of observed grains in each of the grain compartments, tabulated precisely as the generated grains were, i.e., using the same grain compartments and the same mode of grain location.

A source compartment was defined as being

uniformly labeled internally. Therefore, a basic assumption underlying the initial mask tabulation is that the chosen source compartments are indeed uniformly labeled. This assumption is not easy to test, but as will be discussed below, it can be tested in the subsequent analysis if a nonsquare matrix is made. A detailed example of the "mask" analysis can be given from Fig. 7 consisting of two neurons, a Schwann cell, and an axon with a ^{14}C -mask superimposed on it. The source compartments can be neuronal nucleus (Nuc), mitochondria (Mit), other cytoplasm (OCyt), Schwann cell (Sch), and Axon (axon). The grain compartments can be neuronal nucleus (Nuc), mitochondria (Mit), a 1-HD rim around each mitochondria (Mitrym), all other neuronal cytoplasm (OCyt), Schwann cell (Sch), a 1-HD rim around each Schwann cell (Schrim), a zone in the Schwann cell which is within 5 HD of an axon (Schax), the axon (Axon), and a 1-HD rim around the axon (Axonrim). The source compartments were chosen to illustrate different geometric relationships of potentially labeled structures. The grain compartments were chosen for the following reasons. Mitochondria (Mit) are small relative to the resolution of ^{14}C , and because radiation spread outside a radioactive structure is relatively greater for small structures, a rim outside them is used for an additional grain compartment (Mitrym). The neuronal nuclei (Nuc) and Cytoplasm (OCyt) are large relative to the resolution, and we had no rea-

TABLE II *a*
Observed Grains and Generated Source-to-Grain Matrix for Example Analysis (Sample Autoradiograph Illustrated in Fig. 7)

OBSERVED GRAIN DISTRIBUTION									
	NUC	MIT	MITRYM	OCYT	SCH	SCHRIM	SCHAX	AXON	AXONRIM
	11.00	21.00	19.00	24.00	12.00	17.00	7.00	9.00	9.00
GENERATED SOURCE TO GRAIN MATRIX (GRAIN COMP ACROSS)									
	NUC	MIT	MITRYM	OCYT	SCH	SCHRIM	SCHAX	AXON	AXONRIM
NUC	392.00	33.00	81.00	51.00	3.00	2.00	0.0	1.00	1.00
MIT	39.00	91.00	112.00	59.00	12.00	8.00	1.00	0.0	1.00
OCYT	61.00	64.00	71.00	157.00	25.00	14.00	1.00	2.00	3.00
SCH	4.00	10.00	11.00	19.00	39.00	22.00	6.00	5.00	4.00
AXON	3.60	0.70	1.40	4.60	0.70	3.30	3.10	5.90	3.50

Grain compartments are listed across and source compartments are listed down. The number of generated source-to-grain pairs in each matrix element indicates the generated grains in a grain compartment (column) that arises by radiation spread from generated sources in one particular source compartment (row). The observed grains are tabulated in the same compartments as are the generated grains. In using the initial mask tabulation, the number of generated sources that fall in each source compartment is proportional to the size of that compartment (and thus the generated source densities are equal for all source compartments). In the subsequent analyses, the relative extent of label in the different source compartments can be varied either on the basis of some specific hypothesis (Table II *b*), or by the computer until a best fit to the observed grains is obtained (Table II *c*, see also reference 3).

TABLE II b

Grain compartment	Observed grains	Expected grains	χ^2
Nuc	11	16.37	1.76
Mit	21	21.39	0.01
Mitrym	19	27.50	2.63
OCyt	24	22.92	0.05
Sch	12	4.15	14.85
Schrim	17	8.95	7.24
Schax	7	6.98	0
Axon	9	12.88	1.17
Axonrim	9	7.86	0.17
	129	129	$\Sigma\chi^2 = 27.88$

df = 8, $P < 0.005$

Hypothesis: assumed relative source density of Mit = 1; of Axon = 10; of all other source compartments = 0. Normalizing factor for source density = $(\Sigma \text{observed grains})/(\Sigma \text{generated grains}) = 0.218$.

son to believe that they would be excessively radioactive; therefore, they do not need (at least not on the first iteration of the analysis) spill-over rims for radiation spread. The Schax (or Schwann cell within 5 HD from Axon) was chosen because we are assuming in this hypothetical example that we have some previously obtained reason for expecting the axon to be very radioactive. Because Schwann cells are invariably found in the vicinity of axons, heavy radiation spread from a hot axon would make it difficult, even with a 1-HD axonal rim, to determine with any degree of accuracy whether the Schwann cell contains any radioactivity of its own. Thus, the greater subdivision of grain compartments (approaching histogram form) not only aids in determining the specific activity and uniformity of label of a highly radioactive structure, but is very important in assessing the radioactivity of a low activity structure adjacent to a high activity neighbor. The matrix tabulation from many autoradiographs, such as the one illustrated in Fig. 7, is given in Table II a. Of the mask source-to-grain pairs illustrated in Fig. 7, no. 1 is in the source compartment OCyt and in the grain compartment Mitrym, source-to-grain pair no. 7 is in the 'Mit' source compartment and 'axonrim' grain compartment; source-to-grain pairs nos. 2 and 6 are both in the 'Nuc to Nuc' matrix element, etc. Table II a also gives the observed grains seen in the various grain compartments.

If we wished to test a simple hypothesis such as, for instance, that the axon is 10 times more radioactive than the neuronal mitochondria (Mit), and that the other source compartments all had no radioactivity at all, this could be done by a simple χ^2 test (Table II b) as follows: the observed

grains are listed in Table II a. To calculate the expected grains, we first use Eq. 1 of the Appendix and then multiply these expected grains by a normalizing factor so that the total expected grains equal the total observed grain. The resultant χ^2 tabulation, seen in Table II b, leads us to reject our hypothesis ($P < 0.005$). We note that the largest contribution to the total χ^2 comes from the Schwann cell, suggesting that the Schwann cell is labeled. We could now alter our hypothesis repeatedly, assigning different relative source densities to the various source compartments until the expected and observed grains compare favorably.

If the computer program given in the Appendix is used, it does this iteration automatically. The resultant printout giving optimized computed source density,⁵ χ^2 values, and standard errors is

⁵ The optimized computed source density is given in units of generated source density (i.e., computed sources per generated source). It thus gives only the relative radioactivity in different source compartments. For absolute quantitation, the initial generated source density must first be determined. For example, in the mask analysis of the autoradiograph in Fig. 7, before reduction for illustrations the mask provided one source per 28.81 cm^2 and the magnification of the autoradiograph was $\times 20,000$. The generated source density was thus 0.14 generated sources per μm^2 of tissue surface. Table II c gives an optimized "computed" source density for the Schwann cell of 0.30 ± 0.1 . The Schwann cell thus has $(0.3/0.14) = 2.14 \pm 0.71$ optimized sources/ μm^2 of tissue. This value corresponds to the grain density corrected for radiation spread or the quantity "G" referred to in previous publications, e.g., reference 20, p. 151.)

The absolute amount of radioactivity in the tissue can now be calculated from this density of grain origins,

given in Table II c. The legend of that table explains the information provided by the computer program. From Table II c we see that the axon has the highest source density and that the Schwann cell is indeed labeled. If the final total χ^2 even with the computer program had been unacceptably large, then either a necessary source compartment was left out of the tabulation or the underlying assumption of uniform internal label in each source compartment was incorrect. It is then necessary to revise the mask tabulation altering the source compartments until an acceptably low χ^2 is obtained. Such a test for the validity of a source compartment is possible only if there is more than one grain compartment related to this source compartment, i.e., if a nonsquare matrix is made. This is because with a square matrix, a source density can always be chosen so that it yields computed (expected) grains which exactly match the observed grains giving a zero χ^2 . Only with a nonsquare matrix, where some compartments cannot be manipulated independently, can the internal consistency of a given hypothesis be tested.

As indicated, the mask analysis can also be applied to linear source compartments and with histogram columns providing the grain compartments. No such example is given in the present paper, however, as a detailed study in which this procedure is used is in preparation (Salpeter and Kasprzak).

DISCUSSION

The aims of quantitative autoradiography are first, to determine the location of a radioactive source in a tissue and second, to determine the extent of that radioactivity. The analysis of autoradiographs has to contend with two different but overlapping limitations. First, for accuracy in grain counting, exposure times must be chosen to avoid saturation of the emulsion immediately over a radioactive structure. A typical structure is sufficiently small so that only a few developed grains are produced under optimum conditions. Therefore, to achieve statistical significance, numerous autoradiographs and pooling of grain counts are required. Such pooling is based on some initial assumptions regarding homogeneity of the chosen source compartment. Second, because the resolution is limited (i.e. radiation spread is con-

based on the sensitivity of the technique, the specific activity of the radioactive precursors, and the exposure time.

siderable), radioactivity in one source can produce a developed grain on another structure.

In a previous publication, Salpeter and McHenry (20) compared three methods for analyzing autoradiographs which can be summarized as follows: (a) in the "simple grain density" procedure (14), each developed grain is tabulated on the basis of the compartment (e.g. axon) over which its center is located, the total area of the compartment is measured, and results are presented as average number of grains per unit area of the compartment. In this method, no allowance is made for radiation spread, and the assumed source compartments are automatically the same as the chosen grain compartments. (b) In the "probability circle" analysis (10, 15, 23), grains are tabulated both over a potentially labeled structure and within a specific rim outside it. In an elegant refinement, Williams (23) utilized the additional grain compartments situated at the overlap regions between pairs of different source compartments to partially correct for radiation spread between them. (c) In the "density distribution" procedure, grain density histograms are constructed by tabulating grains per unit area at various distances from a potentially labeled structure. In this method, one has many grain compartments for a given source compartment, and the resulting histogram can be compared with a predicted curve chosen from the previously generated families of universal curves to describe the likely distribution of the radioactivity most accurately. However, in this form the method is appropriate only for structures for which families of universal curves can be generated, and cannot easily be used for irregularly shaped interdigitating structures.

The hypothetical grain method of Blackett and Parry (3) eliminated the restriction to regularly shaped structures, by generating hypothetical grains directly on the autoradiographs using a table of computer-generated random directions and distances derived from the integrated universal curve for a point source. This procedure, together with a computer program for minimizing χ^2 , also suggested by Blackett and Parry (3), is well suited to complex, interdigitating structures. The greater accuracy and speed in using the families of expected distributions was traded for the greater flexibility and wider applicability of the hypothetical grains. The application of the hypothetical grain method in its original form required an appreciable amount of labor. The

TABLE II c
Computer Analysis of Data from Table II a

SUMS OF MATRIX COLUMNS									
	NUC	MIT	MITRYM	OCYT	SCH	SCHRIM	SCHAX	AXON	AXONRIM
	499.60	198.70	276.40	290.60	79.70	49.30	11.10	13.90	12.50
RELATIVE GRAIN COMPARTMENT SIZE IN PERCENT									
	34.89	13.88	19.30	20.30	5.57	3.44	0.78	0.97	0.87

SUMS OF MATRIX ROWS					
	NUC	MIT	OCYT	SCH	AXON
	564.00	323.00	398.00	120.00	26.80
RELATIVE SOURCE COMPARTMENT SIZES IN PERCENT					
	39.39	22.56	27.80	8.38	1.87

SUM OF ALL MATRIX ELEMENTS
1431.80

AVERAGE OBSERVED GRAIN DENSITY
0.0901

OPTIMIZED COMPUTED SOURCE DENSITY--NO CONSTRAINTS

	NUC	MIT	OCYT	SCH	AXON				
	-0.0089	0.1467	0.0163	0.2794	1.8025				
ERROR RANGES OF SOURCE DENSITIES									
	0.0106	0.0506	0.0490	0.0978	0.4323				
COMPUTED GRAIN DISTRIBUTION FROM OPT SOURCE DENSITY									
	NUC	MIT	MITRYM	OCYT	SCH	SCHRIM	SCHAX	AXON	AXONRIM
	10.82	18.15	22.46	24.36	14.30	13.48	7.43	12.06	7.61
COMPONENTS OF CHI-SQ FOR EACH GRAIN COMPARTMENT									
	0.00	0.45	0.53	0.01	0.37	0.92	0.02	0.77	0.25
TOTAL CHI-SQUARE									
	3.33								

OPT COMPUTED SOURCE DENSITY (EACH DENSITY >=ZERO)

	NUC	MIT	OCYT	SCH	AXON				
	0.0	0.1434	0.0066	0.3031	1.7041				
ERROR RANGES OF SOURCE DENSITIES									
	0.0114	0.0500	0.0479	0.0993	0.4268				
COMPUTED GRAIN DISTRIBUTION FROM OPT SOURCE DENSITY									
	NUC	MIT	MITRYM	OCYT	SCH	SCHRIM	SCHAX	AXON	AXONRIM
	13.34	17.69	22.25	23.09	14.90	13.53	7.25	11.58	7.34
COMPONENTS OF CHI-SQ FOR EACH GRAIN COMPARTMENT									
	0.41	0.62	0.47	0.04	0.56	0.89	0.01	0.58	0.38
TOTAL CHI-SQUARE									
	3.95								

The sum of a matrix column gives the total generated grains in a grain compartment derived from all source compartments. The sum of a matrix row gives all the generated source-to-grain pairs derived from a given source compartment. The average observed grain density is the total observed grains divided by total generated source-to-grain pairs. The computer varies the relative source density for each source compartment until the resultant number of grains ("computed grain distribution", see Eq. 1 of Appendix) in each of the grain compartments gives the lowest χ^2 when compared with the observed grains in that grain compartment. This gives the "optimized computed source density" (see footnote 5). "No constraints" means that the optimized source density in any compartment is allowed to be either positive or negative. For biological sense, the computer also gives the optimum computed density (≥ 0), i.e., each density constrained to be positive or zero. Standard error ranges for the computed source densities are calculated as given in the Appendix. χ^2 values are given for each of the grain compartments and summed for all of them. The degrees of freedom (df) is the total number of grain compartments minus the total number of source compartments which are allowed to vary and are not constrained to be zero. E.g., in Table II c with no constraints, $df = 9 - 5$ and with constraints, because the nuclear source compartment is constrained to 0, $df = 9 - 4$.

aims of the present study were (a) to construct "masks" (or overlays) to simplify the process of generating predicted grain distributions on individual autoradiographs, (b) to facilitate analysis of the data by devising a fast and simple computer program, and (c) to take into consideration the variations in the universal curves for different energy isotopes. After this study was submitted, but before it was resubmitted in its present revised form, a paper with aims somewhat similar to (a) and (b) above was published by Blackett and Parry (4), and the reader will find much useful advice in their paper.

In both our present paper and Blackett and Parry's 1977 paper (4), overlays are constructed using the integrated universal curve for a point source derived from the resolution studies of Salpeter et al. (17). Both these studies are also based on the idea for EM autoradiographic analysis initiated in the density distribution method (5, 17, 20), and elaborated in the hypothetical grain method (3, 11, 12). In principle, this idea involves hypothesis testing whereby the distributions of observed developed grains in one's autoradiographs are compared with those expected for various defined sources until a "best fit" source is found. This subsequently allows one to determine the extent of radioactivity (from the optimized source density) for each such source compartment. Both mask papers thus have many similarities. However, Blackett and Parry (4) did not take into consideration the varying shapes of the universal curves for different isotopes, and therefore, their sample overlay is applicable only to tritium sources. The adjustment they recommended for isotopes other than tritium involves using different HD values. However, as we show in Fig. 2 of this paper, this would incur considerable error, especially with higher energy isotopes. We therefore used the different universal curves for ^{125}I , ^3H , and ^{14}C to construct the masks for each isotope separately. Each set of masks was also validated to insure against errors in their construction. Finally, Blackett and Parry link their analysis to the probability circle method of Williams (23), whereas we advocate a flexible approach to the mode of grain tabulation and choice of grain compartments.

We provide (in the Appendix) a guide to a computer program which should enable readers with moderate programming experience and with access to a computer to write their own program. Although Blackett and Parry do not publish their

computer guide, it appears, from their discussions, that our two programs for finding the optimized source densities are very similar, but that the two programs for finding the probable error ranges have a different expressed philosophy. Blackett and Parry's program is in principle more accurate, as it can account for statistical errors in the matrix generation. However, we advise using an appreciably larger total number of "generated" grains than "real" observed grains in constructing the matrix, so that most of the statistical errors come from the observed grain sample. When this is done, our program has the advantage of being easy to program and fast to run.

As already indicated in the previous discussion, our overall attitude to autoradiographic analysis is flexibility. The final choice of procedures to be used must be guided by the problem at hand. For instance, if all potential source compartments are large compared with the resolution (and are likely to be uniformly labeled internally), the simple grain density method can be used, as it is simpler than a mask analysis and the errors incurred in its use are small. If only one (or a few) structure of simple shape is suspected of being heavily labeled, the density distribution procedure should be used as it provides a most sensitive test of the assumptions and is both faster and potentially more accurate than a mask analysis. In most other cases (e.g. if one is interested in small or complex interdigitating structures), a mask analysis is called for, but one still should exercise judgment as to which and how many compartments to use. The initial choice of N source compartments is presumably based on biological considerations; the number of different grain compartments, M , should always exceed N , as only then can the assumption of uniform internal label (i.e., correct choice of source compartments) be tested. One standard way to augment the number of grain compartments beyond the N source compartments is to consider the overlap regions between pairs of source compartments as additional grain compartments (as is advocated by Blackett and Parry, 3). This is a useful procedure when N is reasonably small (≤ 4) and no structure is very radioactive. However, if N is very large, the total number of different grain compartments, $N(N + 1)/2$, becomes excessive. In practice, having too many grain compartments is counterproductive because it is important to have at least a few grains in each chosen grain compartment. On the other hand, if one of the source compartments is highly radio-

active (e.g. the axon in our hypothetical example), it is useful to interpose a number of grain compartments in the vicinity of the hot structure such as the extra compartment (Schax) between axon and Schwann cell thus approaching the density distribution method. In this way, a neighboring, less radioactive structure sees very little radiation spread, and its own radioactivity can be more accurately assessed.

The aim of this series of four papers on resolution has been primarily to optimize the information which can be derived from EM autoradi-

ographs. No one type of analysis, however sophisticated, should be applied dogmatically. We urge investigators to select the best method based on the available information on resolution, in order to test simple, well defined hypotheses unique to their particular problem.

We thank Joyce Davis and James Kish for technical assistance, Shelley Salpeter, and Saul Teukolsky, and Len Fertuck for helpful discussions, and Luis Bachmann for the ^{14}C -line source.

This work was supported by grant GM 10422 from the National Institutes of Health.

APPENDIX

BASIS FOR COMPUTER PROGRAM FOR MASK ANALYSIS OF EM AUTORADIOGRAPHS

BRUCE LAND and EDWIN E. SALPETER

As discussed in the text, a computer program is required for many analyses to optimize the source-densities of N source compartments so that the computed grain distribution (grain-numbers in each of M grain-compartments) gives a "best fit" to the observed grain distribution. Some measure of the probable error in each source density is also required. We give notes on the method we devised to help investigators with access to a computing facility write their own computer code. Our method for calculating the standard error of each source density assumed that: (a) at least three to five times as many generated grains as observed were used, so that errors in the generated source-to-grain-matrix are negligible compared with statistical errors in the observed grain-numbers, and (b) the number of observed grains in each grain compartment is larger than unity, and the average number of grains per grain compartment is larger than five, so that Gaussian rather than Poisson statistics can be used.

Let $I = 1, 2, \dots, N$ denote a source bin, and $J = 1, 2, \dots, M$ denote a grain bin with $M \geq N$. The use of the overlays (masks) on autoradiographs furnishes the number of generated grains in each of the matrix elements $\text{SMAT}(I, J)$ connecting I sources to J grains. The number of observed (experimental) grains in grain bin J is denoted as $\text{YOBS}(J)$. Let $D(I)$ denote some

assumed source-density for the I^{th} source. The expected number of grains in bin J [$\text{YCOMP}(J)$] is then computed by the formula

$$\text{YCOMP}(J) = \sum_{I=1}^N \text{SMAT}(I, J)D(I). \quad (1)$$

The χ^2 deviation of the computed from the observed grain distribution is then defined as

$$\chi^2 = \sum_{J=1}^M \{[\text{YOBS}(J) - \text{YCOMP}(J)]^2[\text{YCOMP}(J)]^{-1}\}. \quad (2)$$

The heart of the computer program consists in varying the assumed value of each $D(I)$ until the value of χ^2 in Eq. 2 reaches a minimum. For this purpose, we used a subroutine, ZXMIN, a quasi-Newtonian algorithm for finding the minimum of a function of N variables, from the "IMSL package, Edition 5" (supplied by IMSL, Houston, Tex.), and chose 500 for the maximum allowed number of iterations for each entry into ZXMIN. This subroutine does not require explicit evaluation of first derivatives. For the initial set of values of $D(I)$ we chose to use for each initialized source density $D(I) = D_0$, the average grain density obtained from our autoradiographs in units of the overlay sources as given in Eq. 3.

$$D0 = \left[\sum_{J=1}^M \text{YOBS}(J) \right] \left[\sum_{I=1}^N \sum_{J=1}^M \text{SMAT}(I, J) \right]^{-1} \quad (3)$$

After the required number of iterations, the "best density distribution" can be displayed by printing out (a) the finalized set of source densities $D(I)$ with $I = 1$ to N , (b) the set of predicted grain-numbers $\text{YCOMP}(J)$ with $J = 1$ to M , (c) the contribution to χ^2 from each J component of the sum in Eq. 2, and (d) the total χ^2 value.

To use probability tables for the χ^2 distribution, one needs the "number of degrees of freedom" df. Because the computer is allowed to vary N separate numbers in minimizing the χ^2 (i.e. optimizing each source compartment rather than having a single normalization for all compartments), the correct value of df is $M - N$ (and not $M - 1$ as given by Blackett and Parry, reference 4). When $M = N$ as in a square matrix, there is a set of $D(I)$ which gives expected grain-numbers equal to the observed, and thus gives χ^2 values of zero except for round-off errors. This type of matrix gives a unique mathematical solution for the average site density per source compartment. In this case, with zero

degrees of freedom, there is no test of the null hypothesis.

When $M > N$, as in a nonsquare matrix, in addition to a solution for $D(I)$, one also has a test of the null hypothesis, i.e., the choice of the initial source compartments. If the total χ^2 is so large that the null hypothesis is untenable, then a different set of source compartments is called for. By examining the individual contributions of the χ^2 , it may be possible to select those source compartments needing adjustment.

The subroutine supplied by IMSL does not discriminate against negative values for a finalized $D(I)$, and this may happen in practice for an occasional source compartment (if the actual density is low and some observed grain-numbers had a downward fluctuation). We chose not to allow negative values for any $D(I)$, which we accomplished through the user supplied function subroutine called by ZXMIN (see the schematic flow diagram in Fig. 8). Basically, the main program associates a new variable, $\text{FIX}(I)$, with each $D(I)$, such that a negative value (or a positive value $< 10^{-3}D0$) of $D(I)$ results in $\text{FIX}(I) = 0$. This in turn results in this particular $D(I)$ being held equal to zero when the subroutine ZXMIN is next called. (With this restriction

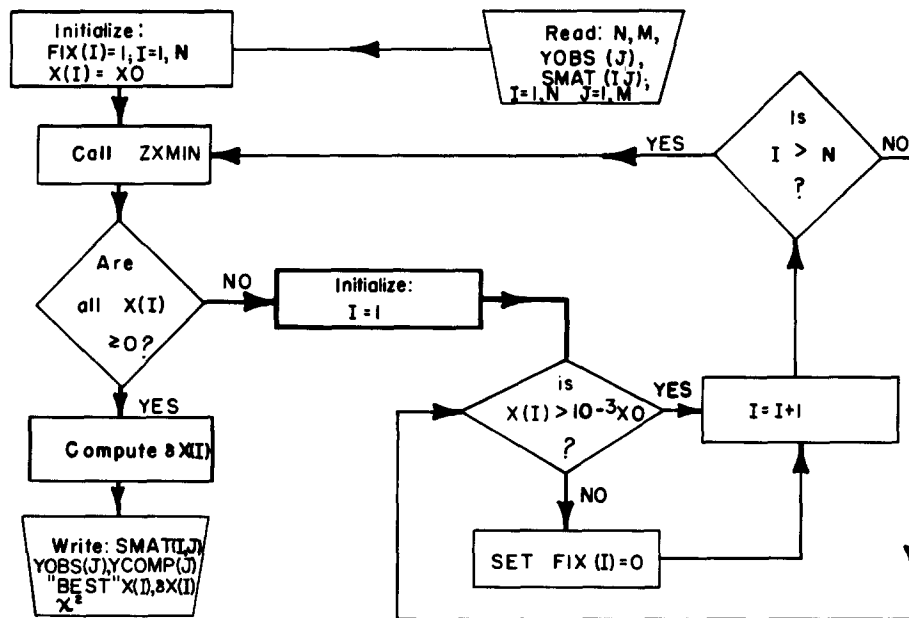


FIGURE 8 Flow chart for computer program.

to positive $D(I)$ the total χ^2 value may be non-zero even for a square matrix.)

If the total χ^2 value obtained is not very much larger than $(M - N)$, then the null hypothesis of source densities $D(1), D(2) \dots D(N)$ cannot be rejected. In this case, one would also like to know how accurate the values of $D(I)$ are likely to be, given the expected fluctuations in $Y(OBS)(J)$ due to the finite sample size, i.e., to obtain some form of standard deviation.

As mentioned, each $YCOMP(J)$ must be larger than unity. Our method is based on the assumption of Gaussian statistics, which is rigorous only if each $YCOMP(J) \gg 1$, but the inaccuracy in our formula for the standard error should be small if the average of $YCOMP(J)$ over all J is larger than about five. The deviation $\Delta(J)$ of $Y(OBS)(J)$ from the correct grain number $Y(J)$ is unknown, but is now assumed to have a Gaussian distribution with mean square equal to $Y(J)$ which we approximated by $YCOMP(J)$. We define a square $N \times N$ matrix $Q(I, K)$ by

$$Q(I, K) = \sum_{J=1}^M \frac{SMAT(I, J)SMAT(K, J)}{YCOMP(J)}, \quad (4)$$

and use a subroutine LINVIF supplied by IMSL to find the inverse square matrix $Q^{-1}(I, K)$. We define next an $N \times M$ matrix $P(I, J)$ by

$$P(I, J) = \sum_{K=1}^N \frac{Q^{-1}(I, K)SMAT(K, J)}{YCOMP(J)}. \quad (5)$$

These matrices Q and P will now be used in the following derivation of the root-mean square error $\delta D(I)$ in the computed density $D(I)$.

We assume throughout that the matrix elements $SMAT(I, J)$ are known exactly and the correct $Y(J)$ would be obtained from Eq. 1 if the correct $D(I)$ were used. In a given experiment, however, one finds $Y(OBS)(J) = Y(J) + \Delta(J)$ with some (unknown) values for $\Delta(J)$. The computer routine assumes densities $[D(I) + \Delta D(I)]$ and varies each $\Delta D(I)$ until χ^2 is a minimum. From the calculus of variations one can show that the final values must satisfy the equations

$$\sum_K Q(I, K)\Delta D(K) = \sum_J Y^{-1}(J)SMAT(I, J)\Delta(J).$$

By means of matrix manipulation these equations can be solved for $\Delta D(I)$; approximating $Y(J)$ by $YCOMP(J)$ in the equations and using the definitions in Eqs. 4 and 5 one finds

$$\Delta D(I) = \sum_J P(I, J)\Delta(J).$$

The value of $\Delta(J)$ in a single experiment is unknown, but its statistical properties are known. Let $\delta D(I)$ be the root-mean square of $\Delta D(I)$, given by

$$[\delta D(I)]^2 = \sum_J \sum_L P(I, J)P(I, L) \langle \Delta(J)\Delta(L) \rangle.$$

Using the fact that different $\Delta(J)$ are uncorrelated and that the mean square of $\Delta(J)$ is approximated by $YCOMP(J)$, one obtains as the desired final expression for $\delta D(I)$, the standard error,

$$\delta D(I) = \left\{ \sum_{J=1}^M [P(I, J)]^2 YCOMP(J) \right\}^{1/2}. \quad (6)$$

After finalized $D(I)$ and $YCOMP(J)$ have been obtained, a computer routine successively evaluates Eq. 4, calls for subroutine LINVIF, evaluates Eqs. 5 and 6, and then prints out our estimate of the probable error $\delta D(I)$ for $I = 1$ to N .

An example of a nonsquare SMAT matrix with five source compartments and nine grain compartments is given in Table II *a* immediately below a set of observed grain numbers $Y(OBS)(J)$. The computer results (after 500 iterations) for this example are given in Table II *b*, including the "best-fit" computed source densities $D(I)$ and the corresponding "standard" error ranges $\delta D(I)$, the finalized computed grains distribution, i.e. each $YCOMP(J)$, the various components of χ^2 , and the total χ^2 . The results are first given without any constraints on $D(I)$, and second, the results are given when the constraint $D(I) \geq 0$ is used for each I .

The total χ^2 value is less than the number of degrees of freedom, $9 - 5 = 4$, and the null hypothesis cannot be rejected. The grain density for $I = 1$ (i.e. nucleus) was put equal to zero by the special $FIX(I)$ subroutine (without it $X(1)$ would have been slightly negative), the source density for $I = 3$ (OCYT) is nonzero by only an insignificant amount, $D(3) < \delta D(3)$; the remaining three source densities (MIT, SCH, and AXON) are each significantly nonzero.

Dr. Land's work was done during the tenure of a research fellowship from the Muscular Dystrophy Association.

Received for publication 5 January 1977, and in revised form 12 August 1977.

REFERENCES

1. BACHMANN, L., and M. M. SALPETER. 1965. Autoradiography with the electron microscope: a quantitative evaluation. *Lab. Invest.* **14**:1041-1053.
2. BACHMANN, L., M. M. SALPETER, and E. E. SALPETER. 1968. Das Auflösungsvermögen elektronenmikroskopische Autoradiographien. *Histochemie.* **15**:234-250.
3. BLACKETT, N. M., and D. M. PARRY. 1973. A new method for analyzing electron microscope autoradiographs using hypothetical grain distributions. *J. Cell Biol.* **57**:9-16.
4. BLACKETT, N. M., and D. M. PARRY. 1977. A simplified method of "hypothetical grain" analysis of electron microscope autoradiographs. *J. Histochem. Cytochem.* **25**:206-214.
5. BUDD, G. C., and M. M. SALPETER. 1969. Distribution of labeled norepinephrine within sympathetic nerve terminals studied with EM autoradiography. *J. Cell Biol.* **41**:21-32.
6. CARO, L. G. 1962. High resolution autoradiography. II. The problem of resolution. *J. Cell Biol.* **15**:189-199.
7. GRANBOULAN, P. 1963. Resolving power and sensitivity of a new emulsion in electron microscope autoradiography. *J. R. Microsc. Soc.* **81**:165-171.
8. GUPTA, B. L., R. B. MORETON, and N. C. COOPER. 1973. Reconsideration of resolution in EM autoradiographs using a biological line source. *J. Microsc. (Oxf.)* **99**:1-25.
9. HAWORTH, R. A., and J. A. CHAPMAN. 1975. ¹²⁵I in electron microscope autoradiography. *Experientia (Basel)*. **31**:258-260.
10. NADLER, N. J. 1971. Interpretation of grain counts in electron microscope radioautography. *J. Cell Biol.* **49**:877-882.
11. PARRY, D. M., and N. M. BLACKETT. 1973. Electron microscope autoradiography of erythroid cells using radioactive iron. *J. Cell Biol.* **57**:16-26.
12. PARRY, D. M., and N. M. BLACKETT. 1976. Analysis of electron microscope autoradiographs using the hypothetical grain analysis method. *J. Microsc. (Oxf.)* **106**:117-124.
13. PELC, S. R. 1963. Theory of electron autoradiography. *J. R. Microsc. Soc.* **81**:131-139.
14. ROSS, R., and E. P. BENDITT. 1965. Wound healing and collagen formation. V. Quantitative electron microscope radioautographic observations of proline-H³ utilization of fibroblasts. *J. Cell Biol.* **27**:83-106.
15. SALPETER, M. M. 1968. H³ proline incorporation into cartilage: electron microscope autoradiographic observations. *J. Morphol.* **124**:387-422.
16. SALPETER, M. M., and L. BACHMANN. 1972. Autoradiography. In Principles and Techniques of Electron Microscopy, M. A. Hayat, editor. Van Nostrand Reinhold Company, New York. **2**:220-278.
17. SALPETER, M. M., L. BACHMANN, and E. E. SALPETER. 1969. Resolution in electron microscope radioautography. *J. Cell Biol.* **41**:1-20.
18. SALPETER, M. M., G. C. BUDD, and S. MATTIMOE. 1974. Resolution in autoradiography using semithin sections. *J. Histochem. Cytochem.* **22**:217-222.
19. SALPETER, M. M., H. C. FERTUCK, and E. E. SALPETER. 1977. Resolution in electron microscopy autoradiography. III. Iodine-125, the effect of heavy metal staining, and a reassessment of critical parameters. *J. Cell Biol.* **72**:161-173.
20. SALPETER, M. M., and F. A. MCHENRY. 1973. Electron Microscope Autoradiography. Analyses of Autoradiograms, In Advanced Techniques in Biological Electron Microscopy. J. K. Koehler, editor. Springer-Verlag New York, Inc., New York. 113-152.
21. SALPETER, M. M., and E. E. SALPETER. 1971. Resolution in electron microscope radioautography. II. Carbon¹⁴. *J. Cell Biol.* **50**:324-332.
22. SALPETER, M. M., and M. SZABO. 1976. An improved Kodak emulsion for use in high resolution electron microscope autoradiography. *J. Histochem. Cytochem.* **24**:1204-1209.
23. WILLIAMS, M. A. 1969. The Assessment of Electron Microscopic Autoradiographs. *Adv. Opt. Electron Microsc.* **3**:219-272.